ELSEVIER

Journal of Alloys and Compounds 253–254 (1997) 302–307

Journal of ALLOYS AND COMPOUNDS

Study of the system $Zr_{1-x}Ti_x(Cr_{0.5}M_{0.4}V_{0.1})_2 - H_2$ ($0 \leq x \leq 0.2$, M=Fe, Co, Ni).

M. Bououdina, P. Menier, J.L. Soubeyroux*, D. Fruchart

Laboratoire de Cristallographie, CNRS, 166X, 38042 Cedex 9, Grenoble, France

Abstract

Alloys of composition $Zr_{1-x}Ti_x(Cr_{0.5}M_{0.4}V_{0.1})_2$ have been synthesised with the hexagonal C14-type Laves phase structure. The crystal structure was studied by the neutron powder diffraction technique. The hydridation properties have been carried out from pressure–composition measurements using a thermogravimetric apparatus. The effects of Zr/Ti and Cr/M substitutions have been studied in view of potential hydrogen storage applications.

Keywords: Metal hydride; Zirconium C14 Laves phase; Neutron diffraction; Crystal structure

1. Introduction

The Laves phase compound $ZrCr_2$ crystallises in the hexagonal C14-type structure. It absorbs and desorbs reversibly a relatively large amount of hydrogen (3.4 H/*f.u.*) [1]. The material was not used for hydrogen storage applications because of its low plateau pressure (1.2 kPa at room temperature) [2]. However the material presents other good hydriding properties. Intensive investigations are now devoted to the substitution of chromium by another transition metal to increase the plateau pressure to suitable values for various applications [2–8].

In a previous study of the system $Zr(Cr,-Co,-V)_2$-H_2 [9], we have shown that the Co/V ratio can modify strongly the hydridation properties by an opposite effect of the two elements (Co decreases the hydrogen capacity and increases the plateau pressure, while V increases the hydrogen capacity and decreases the plateau pressure). In this work, we have chosen an optimized Co/V ratio (=4) and we have analysed the influence of the substitution of zirconium by titanium. In a third step we have used the optimised Ti composition to investigate the system when Co is replaced by another 3d metal (Fe or Ni).

This paper presents the structural parameters of the as cast alloys and their corresponding hydrides determined by means of X-ray and neutron diffraction analysis and the pressure–composition measurements performed by the thermogravimetric method.

2. Experimental details

The $Zr_{1-x}Ti_x(Cr_{0.5}M_{0.4}V_{0.1})_2$ samples for $0 \leq x \leq 0.2$ with M=Fe, Co, Ni samples investigated in this study have been prepared by the HF induction furnace technique using pure starting elements (3N purity). The hydrides with the maximum hydrogen content have been synthesised in a stainless steel container. The hydrogen uptake was determined from the difference in weight before and after the charging procedure [9]. For the neutron experiments, the samples were charged with deuterium.

Both alloys and hydrides were analysed by X-ray powder diffraction technique using a Philips diffractometer (λ=1.5418 Å).

The neutron diffraction experiments were carried out at 280 K at the SILOE reactor of C.E.N.-Grenoble, on the DN5 powder diffractometer, which is equipped with an 800 cells position sensitive detector, covering a $80°–2\theta$ range. The wavelength used was 1.336 Å. The diffraction patterns were analysed by using the FULLPROF profile refinement software [10].

The pressure–composition isotherms (P-C-T) were measured using a thermogravimetric system described previously [11].

*Corresponding author.

0925-8388/97/$17.00
PII S0925-8388(96)02901-5

3. Results and discussion

3.1. Structural parameters

The as-cast alloys of formula $Zr_{1-x}Ti_x(Cr_{0.5}M_{0.4}V_{0.1})_2$ for $0 \leq x \leq 0.2$ and M=Co, Fe, Ni) crystallise in the hexagonal C14-type structure. Table 1 reports the refined cell parameters measured by the X-ray diffraction technique and the corresponding maximum hydrogen content.

In Fig. 1, we have reported the variation of the cell volume alloy versus the titanium composition (curve a) and versus the atomic radius of the substituted element M (curve b). We can notice a decrease of the cell volume when the amount of titanium increases, which is in good agreement with the decrease of the atomic radius. When chromium is replaced by Fe, Co and Ni, we note a decrease in the cell volume according to the atomic radius reduction. These results confirm the substitution of the Ti atoms on the Zr site (4f site) and that of the 3d elements (Fe, Co, Ni) on the Cr sites (2a and 6h sites).

The X-ray diffraction patterns of the hydrides indicate a complete transformation of the alloy into a hydride phase. The crystal structure of the alloy was conserved after hydrogenation. From Table 1 we show that the hydrogen content for all samples is relatively high, H/M =1.07–1.27 H atom/*f.u.* and that the cell volume expansion is greater than 17.8%.

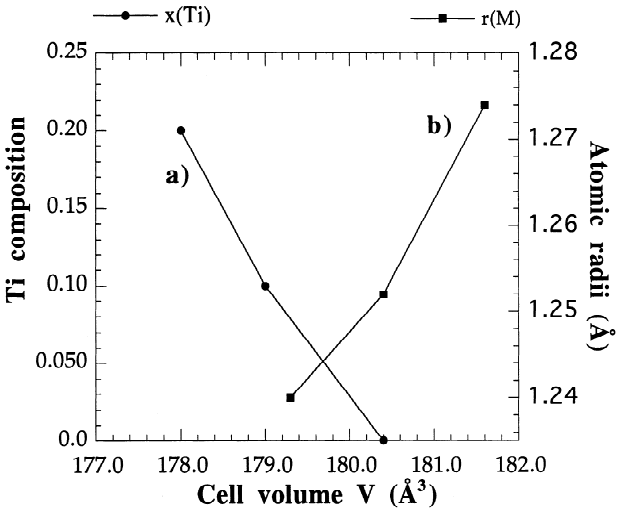

Fig. 1. Variation of the cell volume versus the titanium concentration (curve a) and versus the atomic radius of the substituted metal (curve b).

3.2. Crystal structure refinements

The Rietveld refinement method for the neutron powder diffraction data of the alloys and their corresponding hydrides was used to determine the metal site occupancies and the parameters of the occupied hydrogen interstitial sites. The refinement was carried out by assuming a random distribution of Ti and Zr atoms on the site 4f(A) with $x_{Zr} + x_{Ti} = 1$ and for the Cr-V-Co atoms on the sites 2a and 6h (B) with the constraints: $X^{2a}_{Cr} + X^{2a}_{V} + X^{2a}_{Co} = 0.67$ and $X^{6h}_{Cr} + X^{6h}_{V} + X^{6h}_{Co} = 1.33$. The refinement confirms the hexagonal structure for the as-cast alloy (Fig. 2) and the refined formula is in good agreement with the chemical one (Table 2). The refinements of the deuterides carried out on the $Zr(Cr_{0.5}Co_{0.4}V_{0.1})_2D_y$ and $Zr_{0.9}Ti_{0.1}(Cr_{0.5}Co_{0.4}V_{0.1})_2D_y$ confirm that the hexagonal structure of the parent alloy is conserved (Fig. 3) and that the hydrogen atoms are localised on the A2B2 type of sites in agreement with earlier results [12]. The refined hydrogen site occupancies are reported in the Table 3. We note that the most occupied interstitial site is D1 with 46%, and the lowest one is D4 with less than 5% of the total hydrogen uptake. The broad bump observed at $2\Theta = 37°$ corresponds to short range correlations between deuterium atoms at a 2.1 Å distance [13].

3.3. Phase composition: P-C-T diagrams

On Fig. 4 we have plotted absorption–desorption isothermal curves measured at temperatures within the range 298–423 K. From the investigations of the $Zr_{1-x}Ti_x(Cr_{1-y}Fe_y)_2$ system [14], it was observed that the titanium was playing an important role on the plateau slope, while the iron substitution was mainly affecting the hydride stability and the width of the hysteresis loop.

3.3.1. Effect of titanium substitution

For the $Zr_{1-x}Ti_x(Cr_{0.5}Co_{0.4}V_{0.1})_2$-$H_2$ system, the absorption–desorption isotherms show a decrease of the hydrogen storage capacity with the Ti content. At room temperature, the H/M ratio is decreasing from 1.5 to 1.1 H/*f.u.* The P–C–T curves show an increase of the plateau

Table 1
Cell parameters and hydrogen maximum capacity of alloys and hydrides synthesised in the C14-type structure for the as-cast samples

	Alloys			Hydrides				
	a(Å)	*c*(Å)	*V*(Å^3)	N_H	*a*(Å)	*c*(Å)	*V*(Å^3)	$\Delta V/V$(%)
$Zr(Cr_{0.5}Co_{0.4}V_{0.1})_2$	5.066(4)	8.245(7)	180.4	3.80	5.330(2)	8.720(4)	214.5	18.9
$Zr_{0.9}Ti_{0.1}(Cr_{0.5}Co_{0.4}V_{0.1})_2$	5.014(1)	8.220(2)	179.0	3.60	5.323(1)	8.709(2)	213.7	19.4
$Zr_{0.8}Ti_{0.2}(Cr_{0.5}Co_{0.4}V_{0.1})_2$	5.004(2)	8.210(3)	178.0	3.25	5.290(4)	8.651(8)	209.7	17.8
$Zr_{0.9}Ti_{0.1}(Cr_{0.5}Fe_{0.4}V_{0.1})_2$	5.040(2)	8.260(3)	181.6					
$Zr_{0.9}Ti_{0.1}(Cr_{0.5}Ni_{0.4}V_{0.1})_2$	5.021(2)	8.215(3)	179.3	3.20	5.320(2)	8.710(4)	213.5	19.0

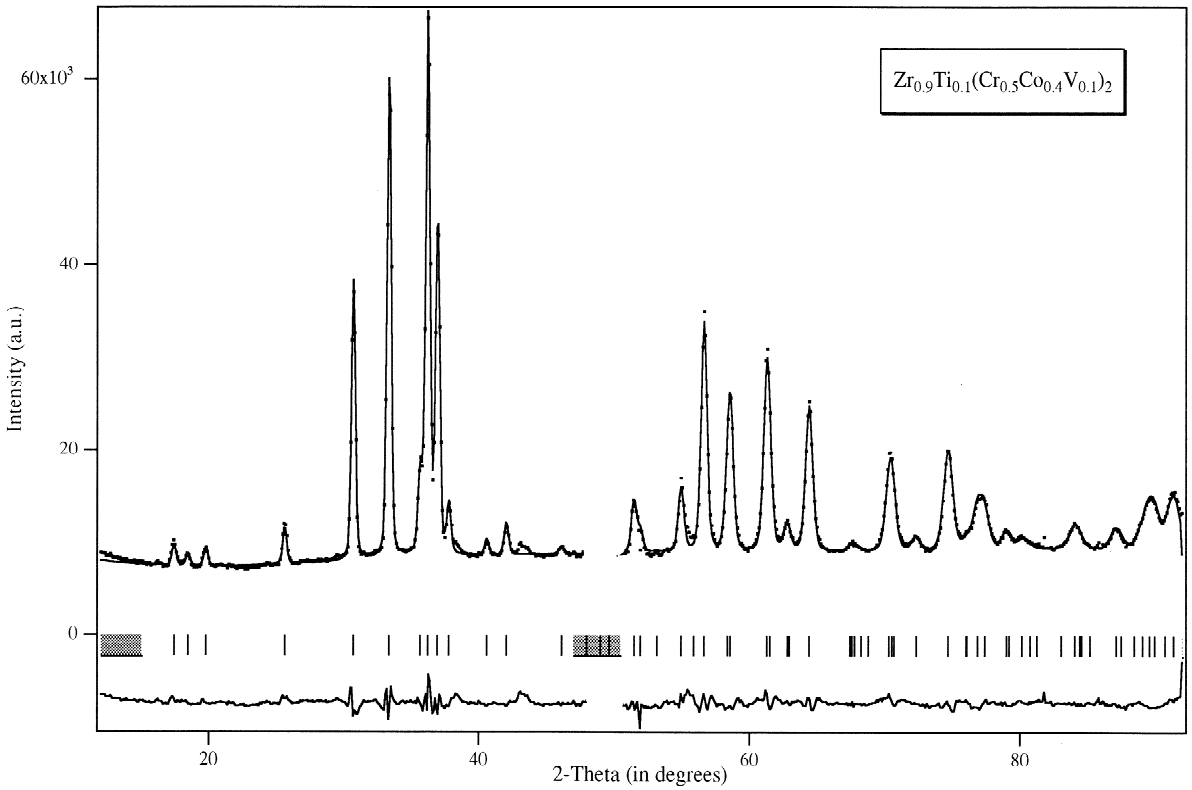

Fig. 2. Powder neutron diffraction pattern of $Zr_{0.9}Ti_{0.1}(Cr_{0.5}Co_{0.4}V_{0.1})_2$ as-cast alloys recorded at $\lambda = 1.336$ Å: °, experimental points; -, calculated intensities; |, line positions. The difference between observed and calculated values is shown at the bottom.

Table 2
Neutron diffraction structure refinement parameters for $Zr(Cr_{0.5}Co_{0.4}V_{0.1})_2$ and $Zr_{0.9}Ti_{0.1}(Cr_{0.5}Co_{0.4}V_{0.1})_2$ as-cast hexagonal C14 type alloys

$P6_3/mmc$	$ZrCr_2$	$Zr(Cr_{0.5}Co_{0.4}V_{0.1})_2$	$Zr_{0.9}Ti_{0.1}(Cr_{0.5}Co_{0.4}V_{0.1})_2$
T(K)	300	280	275
λ(Å)	1.336	1.336	1.336
a(Å)	5.113(2)	5.030(5)	5.075(1)
c(Å)	8.309(3)	8.248(1)	8.302(1)
4f(1/3,2/3,*z*)			
Zr/Ti *z*	0.4374(6)	0.4358(3)	0.4390(3)
*n*Zr	0.167	0.167	0.145(1)
*n*Ti	0	0	0.018(1)
2a(0,0,0)			
*n*Cr	0.0833	0.038(2)	0.041(1)
*n*Co	0	0.037(2)	0.034(1)
*n*V	0	0.012(2)	0.009(1)
6h(*x*,2*x*,1/4)			
Cr/M *x*	0.8196(4)	0.829(1)	0.8301(8)
*n*Cr	0.25	0.129(2)	0.126(1)
*n*Co	0	0.096(2)	0.092(1)
*n*V	0	0.021(2)	0.024(1)
Rp(%)	4.8	12.1	9.21
RWp(%)	7.1	12.5	8.71
RB(%)	12.5	6.84	3.77
2a site		$Cr_{0.23}Co_{0.22}V_{0.07}$	$Cr_{0.25}Co_{0.20}V_{0.05}$
6h site		$Cr_{0.77}Co_{0.58}V_{0.13}$	$Cr_{0.76}Co_{0.59}V_{0.14}$
Refined formula	$ZrCr_2$	$Zr(Cr_{0.5}Co_{0.4}V_{0.1})_2$	$Zr_{0.87}Ti_{0.11}(Cr_{0.5}Co_{0.4}V_{0.1})_2$

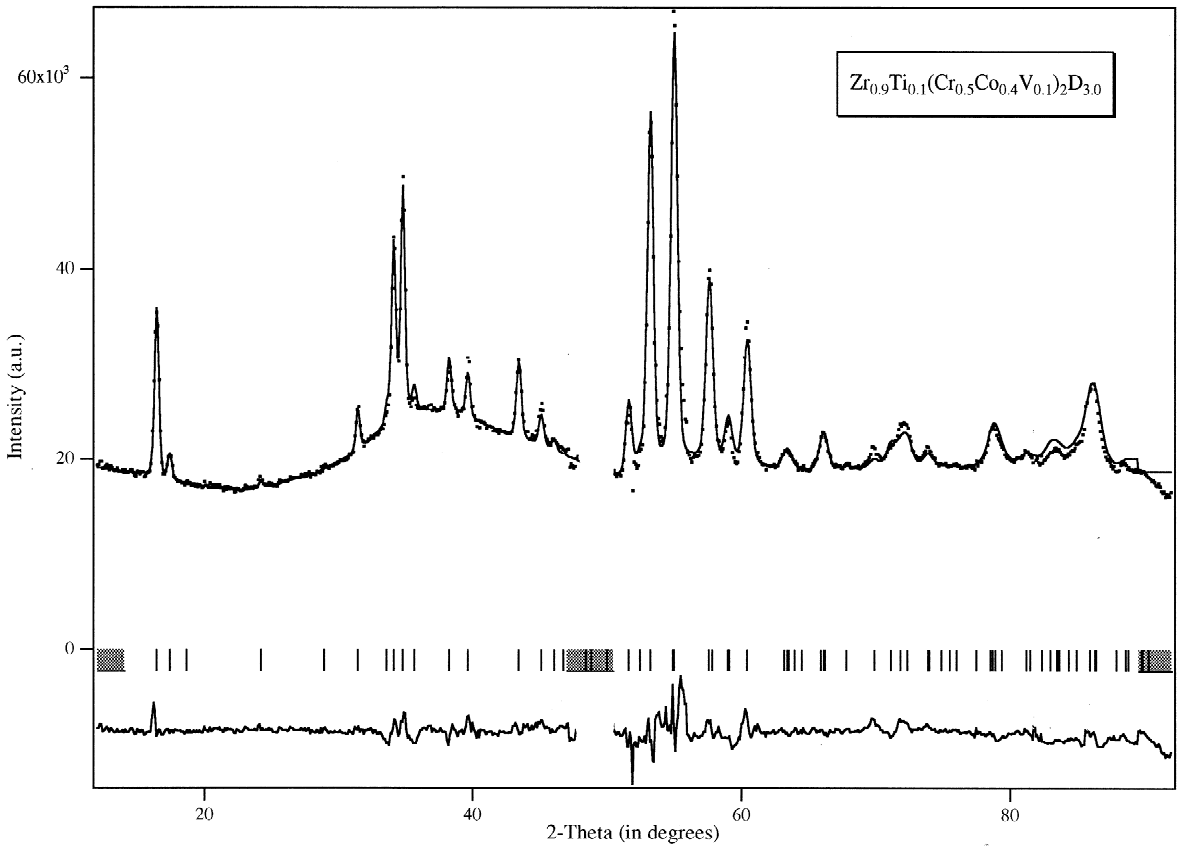

Fig. 3. Powder neutron diffraction pattern of $Zr_{0.9}Ti_{0.1}(Cr_{0.5}Co_{0.4}V_{0.1})_2D_3$ deuteride recorded at $\lambda = 1.336$ Å.

pressure corresponding to a reduction in the hydride stability. At room temperature, only 0.17 H/*f.u.* can be recovered at desorption for the composition without Ti, whereas for $x(\mathrm{Ti}) = 0.1$, the amount of the released hydrogen is H/M = 0.3 H/*f.u.*

In the temperature range studied, all plateaus are sloped. The slope increases as zirconium is partially substituted by titanium, for $x(\mathrm{Ti}) = 0.2$ and at 423 K, the plateau disappears.

From the width of the hysteresis loop, we note a gradual decrease of the hysteresis with temperature for $x(\mathrm{Ti}) = 0$. For the compound with $x(\mathrm{Ti}) = 0.1$, the hysteresis effect is relatively weak and it seems unaffected by temperature. For $x(\mathrm{Ti}) = 0.2$, we note an increase of the hysteresis with temperature.

3.3.2. Effect of the transition metal substitution

For the nickel substitution the P–C–T curve recorded at room temperature indicates a hydrogen capacity H/M = 1.17 but H/M = 0.97 at 348 K. For the iron substitution, we note an increase of the capacity, at 348 K the ratio H/M is equal to 1.07. At the same temperature, for the cobalt system, the H/M ratio is also 1.07.

The hysteresis width is very narrow for the cobalt compound, but it becomes wider and more apparent for iron and nickel. For the Fe and Co substitutions, the P–C–T curves indicate a decrease of the hysteresis width with temperature.

Concerning the hydrides stability, we have determined the amount of hydrogen reversibly absorbed (δ), the ratio H/M was measured at the end of the desorption. We have

Table 3
Hydrogen interstitial sites occupancy factors for $Zr(Cr_{0.5}Co_{0.4}V_{0.1})_2D_y$ and $Zr_{0.9}Ti_{0.1}(Cr_{0.5}Co_{0.4}V_{0.1})_2D_y$ samples as obtained from neutron diffraction refinements

	*D*1(24l)	*D*2($12k_2$)	*D*3($6h_1$)	*D*4($6h_2$)	N_H (H/AB_2)
$Zr(Cr_{0.5}Co_{0.4}V_{0.1})_2$	1.39(3)	0.94(3)	0.56(3)	0.13(1)	3.02
$Zr_{0.9}Ti_{0.1}(Cr_{0.5}Co_{0.4}V_{0.1})_2$	1.43(3)	0.94(3)	0.57(3)	0.16(1)	3.10

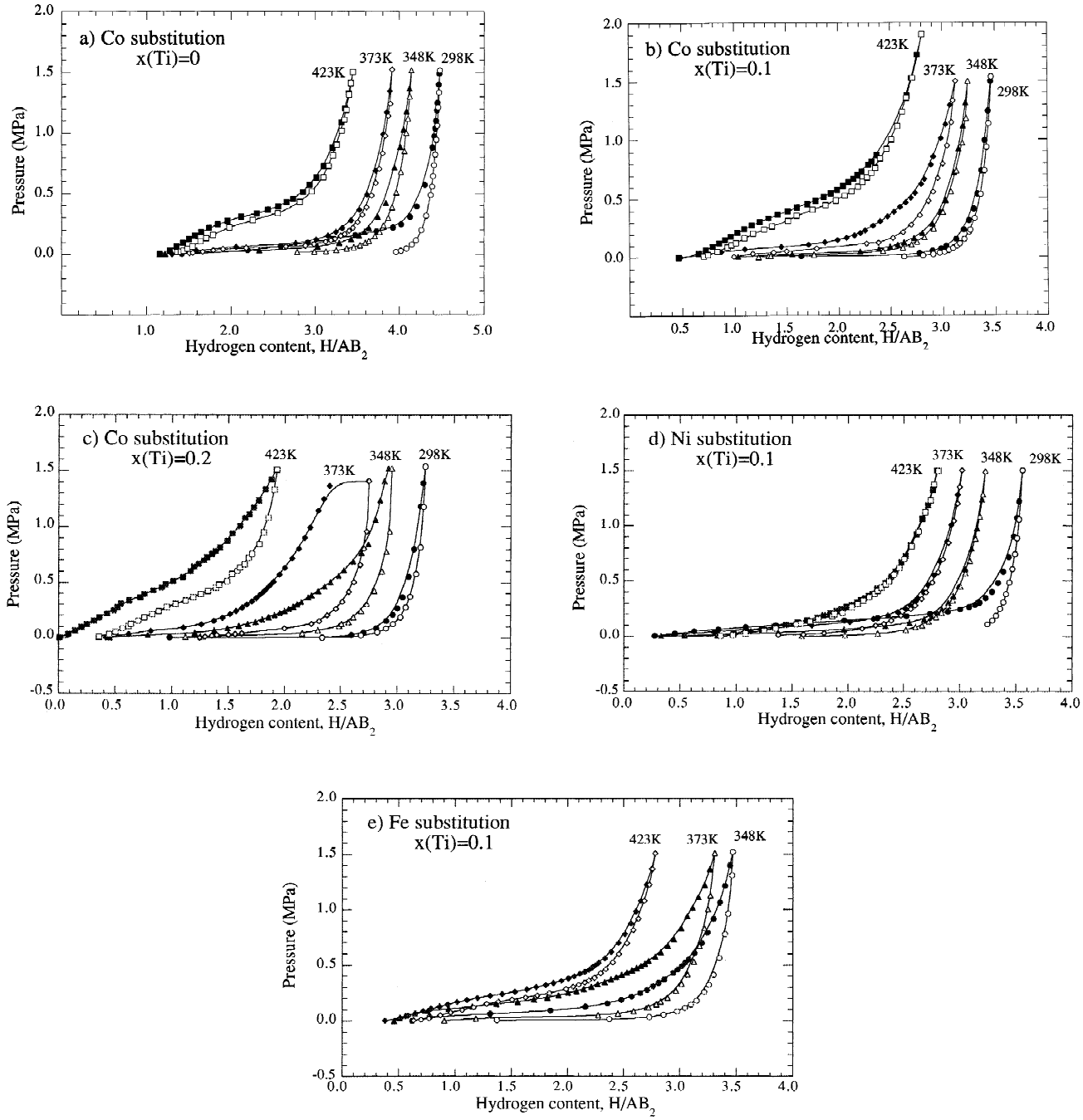

Fig. 4. Pressure–composition isotherms recorded in the temperature range 298–423 K for different compositions (the open symbols are for absorption isotherms and the closed ones are for the desorption isotherms).

found 0.70, 0.67 and 0.53, respectively, for Fe, Co and Ni. This indicates an increase of the hydride stability with the atomic number *Z* of the transition metals.

From the P–C–T curves, we also notice a decrease of the plateau pressure when cobalt is replaced by iron or nickel. However, the plateau pressure for the iron compound is higher than for the nickel one. In all cases, the plateaus are not well-defined and it is difficult to extract information on the plateau slope.

4. Conclusion

Compounds of formula $Zr_{1-x}Ti_x(Cr_{0.5}M_{0.4}V_{0.1})_2$ have been synthesised with the C14 hexagonal type of Laves phases. They absorb hydrogen and the capacity at room temperature is very high. We have noticed that $Zr_{0.9}Ti_{0.1}(Cr_{0.5}Co_{0.4}V_{0.1})_2$ absorbs hydrogen readily at room temperature under 500 kPa. The P–C–T diagrams reveal that the substitution of a limited amount of zir-

conium by titanium reduces the hydride stability while preserving a relatively good hydrogen capacity. Moreover, we have observed that the substitution of chromium by nickel simultaneously reduces the hysteresis width and the plateau slope. Nevertheless, at 348 K, Ti and Ni substituted compounds present a good hydrogen content ($H/M > 1.0$), a low hysteresis and form a rather stable hydride.

References

[1] A. Pebler and E.A. Gulbransen, *Electrochem. Technol., 4* (1966) 211.
[2] D. Shaltiel, I. Jacob and D. Davidov, *J. Less-Comm. Met., 53* (1977) 117.
[3] S. Qian and D.O. Northwood, *J. Less-Comm. Met., 147* (1989) 149.
[4] M. Boulghallat, N. Gerard, O. Canet and A. Percheron-Guegan, *Z. Phys. Chem. NF, 179* (1993) 171.
[5] A. Drasner and Z. Blazina, *J. Less-Comm. Met., 163* (1990) 151.
[6] A. Drasner and Z. Blazina, *J. Less-Comm. Met., 175* (1991) 103.
[7] A. Drasner and Z. Blazina, *J. Alloys Comp., 199* (1993) 101.
[8] M. Bououdina, P. De Rango, J.L. Soubeyroux, D. Fruchart, E. Akiba and K. Nomura, *J. Alloys Comp., 253–254* (1997).
[9] M. Bououdina, J.L. Soubeyroux, D. Fruchart, E. Akiba and K. Nomura, *J. Alloys Comp., 235* (1996) 93.
[10] J. Rodriguez-Carvajal, *Proc. XVth Congr. Int. Union of Crystallography, Satellite Meeting on Powder Diffraction*, Toulouse, 1990, p. 127.
[11] M. Bououdina, J.L. Soubeyroux, P. Juen, C. Mouget, R. Argoud and D. Fruchart, *J. Alloys Comp., 231* (1995) 422.
[12] J.L. Soubeyroux, M. Bououdina, D. Fruchart and L. Pontonnier, *J. Alloys Comp., 219* (1995) 48.
[13] J.L. Soubeyroux, L. Pontonnier, S. Miraglia, O. Isnard, D. Fruchart, E. Akiba, H. Hayakawa, S. Fujitani and I. Yonezu, *Z. Phys. Chem. NF, 179* (1993) 188.
[14] J.M. Park and J.Y. Lee, *J. Less-Comm. Met., 160* (1990) 259.